Molecular Vision 2007; 13:1822-7 <http://www.molvis.org/molvis/v13/a203/>
Received 27 July 2007 | Accepted 28 September 2007 | Published 30 September 2007

A substitution of arginine to lysine at the COOH-terminus of MIP caused a different binocular phenotype in a congenital cataract family

Hui Lin,[1,2] J. Fielding Hejtmancik,[2] Yanhua Qi[1]

[1]Department of Ophthalmology, the Second Affiliated Hospital, Harbin Medical University, Harbin, China; [2]Ophthalmic Genetics and Visual Function Branch, National Eye Institute, National Institutes of Health, Bethesda, MD

Purpose: To detect the cataractogenetic mutation for a six-generation family of Chinese origin with autosomal dominant binocular polymorphic cataracts.
Methods: A genome wide scan was performed using 382 fluorescent-labeled microsatellite markers. Multiple polymerase chain reaction (PCR) was performed according to the protocols previously described. Two-point linkage analysis was performed with the FASTLINK version of the MLINK in Linkage Program Package. The candidate gene was screened by direct sequencing.
Results: The disease locus was mapped to a 61 cM region on chromosome 12 defined by D12S310 and D12S351 near the major intrinsic protein gene (*MIP*). The maximum two-point lod score of 5.44 was obtained at marker D12S83 at θ=0.00. Direct sequencing of the encoding region of the candidate gene revealed a novel missense mutation G>A in exon 4 at nucleotide 702, which caused the replacement of arginine to lysine at codon 233 (p.R233K).
Conclusions: The change located in the α-helix domain of the COOH-terminus of MIP was determined to be associated with the binocular polymorphic cataract in this study. It suggests that arginine in this domain plays a crucial role in the function of the carboxyl-end of this protein and provides a helpful clue to further studies on completely understanding the physiological significance of *MIP* and its role in the formation of cataract.

Aquaporins are members of the water channel superfamily of transmembrane proteins. So far, 13 homologs of aquaporins have been identified [1,2]. Major intrinsic protein (MIP), also called aquaporin 0, is a member of aquaporins known to function as the lens-specific water channel [3]. It is predominantly expressed in lens and is the most abundant membrane protein present in lens fiber cells [4]. It is enriched in both the nonjunctional regions in the plasma membranes [5] and the 11-13 nm thin junctions between lens fiber cells [6], which indicates that MIP also acts as an adhesion molecule [7].

The question as to the main function of MIP has been debated throughout its research history. Recent data from Gonen et al. [7,8], however, presented a new perspective on these two roles. They proposed that MIP principally performed the function of water pores in the lens cortex. In the lens core, thin junctions were formed between MIP molecules in adjoining membranes of lens fiber cells to make the tight packing of the fiber cells. Consequently, water pores in junctional conformation were closed. The other nonjunctional MIP in the lens core retained their properties of water conductance and became more active than in the cortex, offseting the functional loss of the junctional fraction.

Correspondence to: Yanhua Qi, Department of Ophthalmology, the Second Affiliated Hospital, Harbin Medical University, Harbin, China, 246 Xuefu Road, Harbin, China, 150086; Phone: 0451-86605643; FAX: 0451-86605116; email: qi_yanhua@yahoo.com

These studies imply that MIP served complementary dual physiological functions in the lens and played a paramount role in maintaining lens transparency.

Two missense mutations in exon 2 of *MIP* (T138R and E134G) have been associated with a polymorphic cataract family and a lamellar cataract family, respectively. The former commonly showed discrete bilateral punctuate lens opacities. Some had asymmetric anterior and posterior polar opacification. The latter had lamellar and sutural cataract. MIP has been predicated to consist of six transmembrane helices. The two mutations were located in transmembrane domain 4. They were thought to change amino acid hydrostatic charge and size. Consequently, the water channel might fail to form in the cell membrane, and water transportation might be disrupted [9]. One single-base pair deletion at nucleotide 3,223 of exon 4 was reported to cause polymorphic bilateral cataract with radiating, vacuolar or dense opacities in the embryonal nucleus and fine punctate opacities in different posterior cortical locations. This mutation produced the 257 amino acid truncated MIP protein that probably altered calmodulin-binding properties of the COOH-terminus [10].

We herein present a six-generation congenital cataract Chinese family with a rare polymorphic phenotype associated with a novel missense mutation in *MIP* demonstrating different cataract morphologies in the binocular lens.

METHODS

Genetic materials: The six-generation family enrolled in this

study was found in a northeast province of China (Heilongjiang). Clinical examination, peripheral blood collection, and DNA extraction were performed in the Department of Ophthalmology, the Second Affiliated Hospital of Harbin Medical University. Informed consent in accordance with the Declaration of Helsinki and the Institutional Review Board and Ethics Committee of Heilongjiang province was obtained from all participants. Twenty-eight individuals were available from the original family with an inherited pattern of autosomal dominant cataract including 12 affected members (Figure 1). Clinical data of these subjects were ascertained by case records of surgeries and detailed ocular examinations including the visual acuity test, anterior segment examination by slit lamp, and fundus examination by ophthalmoscope.

Genome wide scan and linkage analysis: We performed a genome wide scan for this family using 382 fluorescent labeled microsatellite markers distributed at an average interval of 10 cM from ABI Prism Linkage Mapping Sets Version 2.5 MD-10 (Applied Biosystems, Foster City, CA). Multiple polymerase chain reactions (PCR) and conditions were performed according to the protocols previously described in detail [11]. PCR products were electrophoresed in the ABI 3100 Genetic Analyzer. The genotyping data were collected by ABI 3100 Genetic Analyzer Data Collection Software v2.0 and were analyzed using ABI Prism GeneMapper software v3.5. Two-point linkage analysis was performed with the FASTLINK version of the MLINK in Linkage Program Package [12], and we modeled cataract in this family as a full penetrance of autosomal dominant trait. The allele frequencies of the disease and all markers were set as 0.0001 and equal frequencies with ten alleles.

Candidate gene screening: A known cataract candidate gene within the linked region, major intrinsic protein (*MIP*), was screened directly. PCR primers were designed for amplifying four exons and flanking intronic sequences (Table 1). The PCR reaction cocktail was a 20 μl mixture containing 80 ng genomic DNA, 10 pmol primer pairs, 200 μmol/l dNTP mix, 1.5 mmol/l $MgCl_2$, 2 μl of 10X PCR Buffer, and 0.2 U Ampli*Taq* Gold DNA Polymerase. PCR cycling conditions consisted of the following: an initial denaturation at 95 °C for

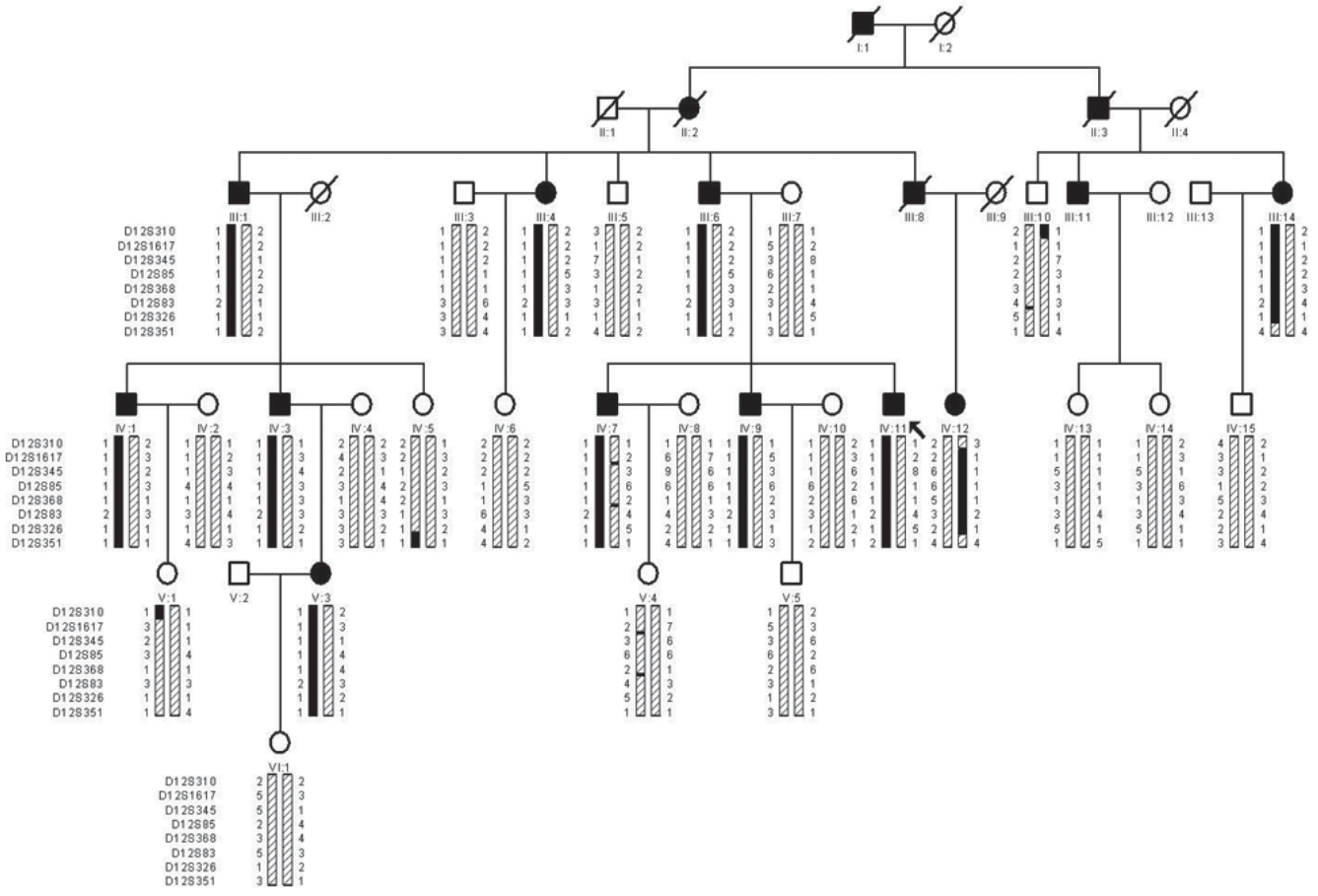

Figure 1. Pedigree and haplotype of the family. A six-generation pedigree with 12 available affected members (indicated by the black symbols) is shown. IV:11 was the proband, which is indicated by the black arrow. Eight markers spanning the centromere were arrayed on the left in the genetic order on chromosome 12. The disease haplotype (represented by the black bar) cosegregated with all affected members from marker D12S1617 to D12S326 but was not shared with unaffected members. The obligate recombination occurred at the boundary markers, D12S310 and D12S351.

8 min, 30 cycles of denaturation at 94 °C for 30 s, annealing at 58 °C for 30 s, extension at 72 °C for 50 s, a final extension at 72 °C for 7 min, and a last hold at 4 °C. The PCR products were purified by a Beckman Biomek NX Laboratory Automation Workstation (Fullerton, CA) with AmPure and CleanSeq reagents then sequenced by ABI 3130xl Genetic Analyzer. DNASTAR software was used for reading and analyzing the sequencing results. All affected members and 50 unrelated normal Chinese controls were screened when the mutation was identified in exon 4.

The reference cDNA (CCDS8919.1), protein (NP_036196), and genomic sequence (NC_000012) are available from the related resource of the National Center for Biotechnology Information (NCBI).

RESULTS

Clinical phenotype: We described the phenotype of the family as polymorphic cataract that was present at birth. It was displayed not only among the members of the family but in the bilateral lens of each individual. All of the affected except for individual IV:7 showed fine white punctate opacities within the posterior cortex of the right lens and anterior polar cataract in the left lens (Figure 2A,B). On the other hand, indi-

Table 1. Polymerase chain reaction primers for sequencing *MIP*

Primer name	Primer sequence (5'-3')	Product size (bp)
Exon-1	Forward GACTGTCCACCCAGACAAGG	493
	Reverse GTCAGGGAGTCAGGGCAATA	
Exon-2	Forward GGGGAAGTCTTGAGGAGGTAA	300
	Reverse AAAGTTGGGAAAGGTTTAGGG	
Exon-3	Forward GAGAAGCTGGGGTGCAGTAG	196
	Reverse AACCTGCAGTCCACAACCAT	
Exon-4	Forward CCACTAAGGTGGCTGGAAAA	360
	Reverse ACCCTCCCCACAGTCTCTTT	

Forward and reverse primers were used to amplify 4 exons of *MIP*. The expected size of PCR products is shown.

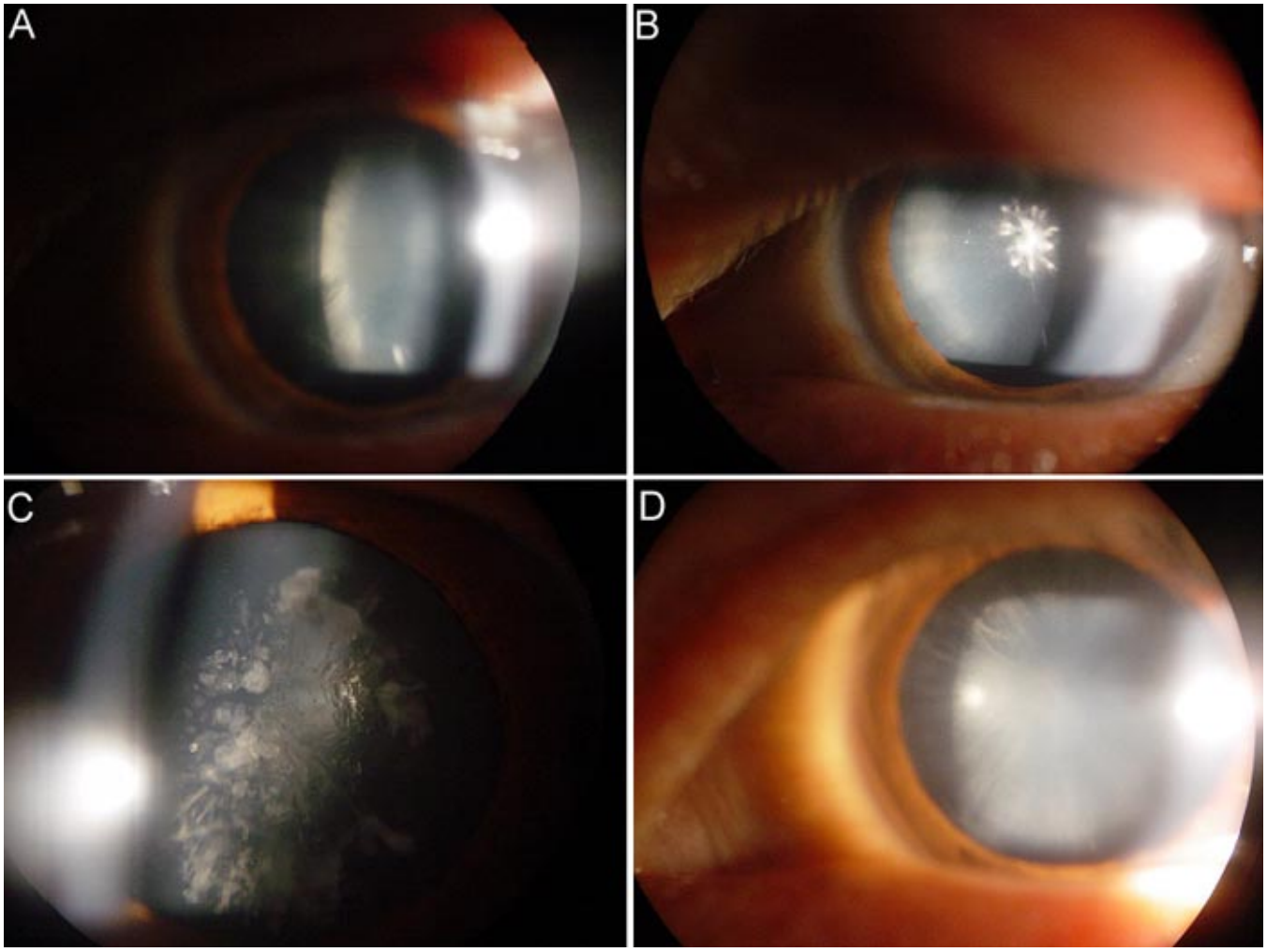

Figure 2. Binocular slit lamp photographs of the affected individuals. **A**: The right eye of individual IV:9 shows fine punctate opacities in the posterior cortex. **B**: The left eye of individual IV:9 shows the anterior polar cataract with punctate opacities in the anterior cortex. **C**: The right eye of individual IV:7 shows fine punctate opacities in the cortex and core of the lens. **D**: The left eye of individual IV:7 shows a mass of irregular opacification clustering in the anterior cortex.

vidual IV:7 presented fine white punctate opacification distributed over the whole left lens and a mass of irregular opaque pieces localized in the anterior subcapsular cortex of the right lens (Figure 2C,D). No affected members except III:6 and the proband (IV:9) underwent an operation. These two patients had cataract surgeries as adults. There was no complaint of distinctly decreased visual acuity with age from all patients.

Linkage results and haplotype: A maximum lod score (Z_{max}=5.44) was obtained at marker D12S83 with the recombination fraction θ=0.00 after the initial genome wide scan. High lod scores were also detected at the markers above D12S83 including D12S85 (Z_{max}=5.22 at θ=0.00), D12S345 (Z_{max}=4.34 at θ=0.00), and D12S1617 (Z_{max}=3.53 at θ=0.00). D12S368 is also a suggestive marker with a Z_{max} value of 2.81 at θ=0.05 (Table 2). These data from two-point linkage analysis strongly demonstrated that the disease locus of the family was mapped to a huge region flanked by D12S310 and D12S351 at 12p11.2-q15, revealing an interval of 61.0 cM, spanning the centromere.

The results of linkage analysis were entirely supported by the haplotypes for markers in this region (Figure 1). The disease allele cosegregated with all affected members at the markers with an lod score greater than two. None of the unaffected individuals shared the same haplotype. Recombination events occurred at boundary markers, D12S310 and D12S326.

Mutation analysis: We predicted *MIP* as a cataract candidate gene between D12S83 and D12S368 within the aforementioned linked area. Direct sequencing of a total of four exons of *MIP* revealed a missense mutation, G>A, at nucle-

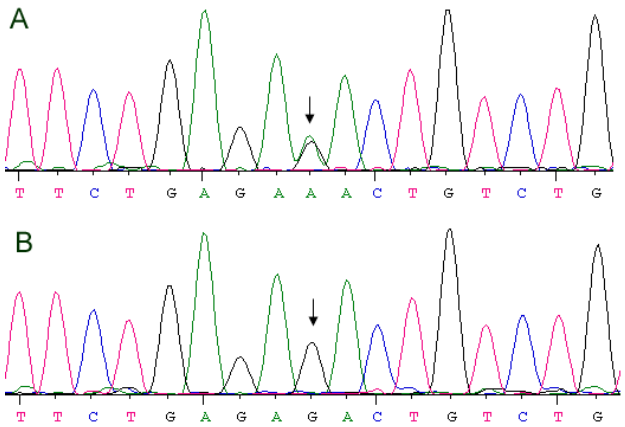

Figure 3. The results of sequencing exon 4 of the major intrinsic protein gene. **A**: A heterozygous change, G>A, denoted by the arrow was found at nucleotide 702 in exon 4 of the affected member (the proband individual IV:11) **B**: A homozygous nucleotide G (denoted by the arrow) was found at the same place in exon 4 of the unaffected member (individual V:4).

Table 2. LOD score table of two-point linkage analysis of eight markers on chromosome 12, arrayed in the genetic order according to the Genethon Map

		Lod score (θ=)								
Markers	Position (cM)	0	0.01	0.05	0.1	0.2	0.3	0.4	Zmax	θ=
D12S310	36.1	-?	-1.59	0.1	0.71	0.93	0.65	0.2	0.93	0.20
D12S1617	45.1	3.53	3.48	3.28	3.02	2.43	1.72	0.91	3.53	0.00
D12S345	54.5	4.34	4.26	3.93	3.51	2.67	1.76	0.77	4.34	0.00
D12S85	62.7	5.22	5.17	4.89	4.48	3.51	2.39	1.14	5.22	0.00
D12S368	67.3	2.23	2.54	2.81	2.76	2.33	1.66	0.84	2.81	0.05
D12S83	76.5	5.44	5.34	4.95	4.43	3.32	2.13	0.91	5.44	0.00
D12S326	87.6	0.87	0.88	0.89	0.84	0.65	0.43	0.2	0.89	0.05
D12S351	97.1	-?	-4.00	-1.40	-0.45	0.23	0.37	0.26	0.37	0.30

This table shows the two-point LOD scores of 8 markers close to *MIP*. A maximum Lod score (Z_{max}=5.44; θ=0.00) was obtained at maker D12S83. Higher LOD scores were also detected at the makers D12S85, D12S345, D12S1617, and D12S368.

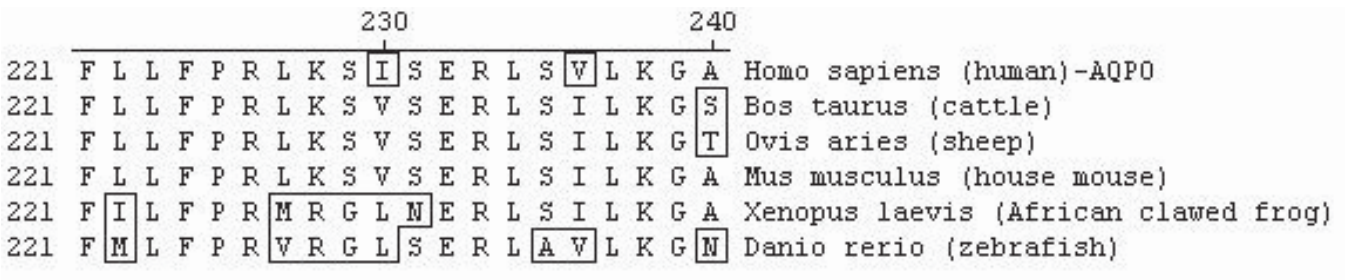

Figure 4. Alignment of amino acid residues from six species. The analysis of the alignment of 20 amino acid residues from 221 to 240 at the COOH-terminus of MIP illustrated that arginine at codon 233 was conserved. The alignment was made up from six different species. The residues that differed from others were circled by the box.

otide 702 (CCDS8919.1) in exon 4 (Figure 3A), resulting in a substitution of arginine to lysine at codon 233 (p.R233K; NP_036196). The transversion mutation cosegregated with all affected members of the family, but was absent in the unaffected offspring and 50 identically ethnic, normal controls (Figure 3B). There was no such sequence alteration in *MIP* present in the dbSNP database at NCBI.

DISCUSSION

We identified the missense mutation G>A the genomic sequece at nucleotide 3,270 (NC_000012) and the cDNA sequence at nucleotide 702 (CCDS8919.1) in exon 4, causing a change of arginine to lysine at codon 233 lying in the COOH-terminus of MIP that included 263 amino acid residues (NP_036196).

Arginine and lysine are both polar and positively charged amino acids. Arginine has a vital impact on the conformation and function of proteins. There are multiple amino groups at the end of the arginine side chain which are involved in making multiplex hydrogen bonds with negatively charged amino acids or other nonprotein anionic atoms. Thus, arginine quite frequently lies in the active or binding sites of the protein. Although lysine also creates interactions with anions, it has only a single amino group at the end of its side chain, which means less hydrogen bonds. Therefore, the supersedure of arginine to lysine may predicate the weakening of the stabilized structure or important function of protein.

Furthermore, alignment analysis of amino acid sequences of MIP from six species (Figure 4) implied that the residue arginine in this region was conservative.

Previous studies suggested that the COOH-terminal of MIP was 44 amino acids long, starting at residue 220 [13] and containing an α-helical key domain from residue 230 to residue 238. The residues between 223 to 235 were known to be the calmodulin-binding site [14,15]. The water permeability of MIP could be modulated by the alteration of the Ca^{2+} concentration through the mediation of calmodulin binding to the α-helix domain [16-18]. The changed arginine at codon 233 was located in both the binding site and the core of the α-helical domain [8]. Accordingly, we presumed that the mutation was likely to influence the binding function of the carboxyl tail as a result of the reduced number of hydrogen bonds.

In addition, the carboxyl end of MIP played important roles on other functions of the protein as well. The experiments of Yu et al. [19,20] showed that the COOH-terminal had a significant effect on the differentiation and maturation of the connexin 45.6 protein during the lens development by dint of the interaction between the intracellular loop of connexin 45.6 and the COOH-terminus of MIP. However, the binding sites have to be identified. Again, residue serine 235 has been determined to be a major phosphorylation site in the COOH-terminus. The role of this post-translational phosphorylated modification remains to be demonstrated [13,21-23]. Hence, this identified mutation might provide a new clue for further studies on fully understanding the functions of the COOH-terminus of MIP.

Congenital cataracts correlated with mutations in *MIP* are commonly known as polymorphic. The family we identified had an unusual polymorphic phenotype in comparison with the families mentioned in the introduction section. It represented different cataract morphologies among the familial individuals even exhibiting distinctly clinical varieties in the binocular lens of each individual. Extensive clinical and genetic heterogeneity of cataract is validated once more. Nevertheless, the potential mechanism of it remains to be elucidated. Like that single base pair deletion, this missense mutation also lay in the last exon of *MIP* [10]. It seems that the relevant mutant protein had the same effect on the function of the COOH-terminal as that shortened protein.

In summary, the mutation detected in the family induced a binocular polymorphic cataract, which increases the clinical heterogeneity of inherited cataract. The replacement between two amino acid residues of analogic properties, arginine and lysine, suggested that arginine might significantly impact the action of the key domain of the carboxyl end. This study contributed a novel missense mutation of *MIP* to the hererogeneity of genetic cataract.

ACKNOWLEDGEMENTS

We are grateful to all the members of this family for agreeing to participate in the study and all the people who helped us complete the research successfully. This research was supported by the National Basic Research Program of China (973 Program 2005 CB724302).

REFERENCES

1. Hibuse T, Maeda N, Nagasawa A, Funahashi T. Aquaporins and glycerol metabolism. Biochim Biophys Acta 2006; 1758:1004-11.
2. Yang B, Verkman AS. Water and glycerol permeabilities of aquaporins 1-5 and MIP determined quantitatively by expression of epitope-tagged constructs in Xenopus oocytes. J Biol Chem 1997; 272:16140-6.
3. Varadaraj K, Kushmerick C, Baldo GJ, Bassnett S, Shiels A, Mathias RT. The role of MIP in lens fiber cell membrane transport. J Membr Biol 1999; 170:191-203.
4. Yancey SB, Koh K, Chung J, Revel JP. Expression of the gene for main intrinsic polypeptide (MIP): separate spatial distributions of MIP and beta-crystallin gene transcripts in rat lens development. J Cell Biol 1988; 106:705-14.
5. FitzGerald PG, Bok D, Horwitz J. The distribution of the main intrinsic membrane polypeptide in ocular lens. Curr Eye Res 1985; 4:1203-18.
6. Costello MJ, McIntosh TJ, Robertson JD. Distribution of gap junctions and square array junctions in the mammalian lens. Invest Ophthalmol Vis Sci 1989; 30:975-89.
7. Gonen T, Sliz P, Kistler J, Cheng Y, Walz T. Aquaporin-0 membrane junctions reveal the structure of a closed water pore. Nature 2004; 429:193-7.
8. Gonen T, Cheng Y, Kistler J, Walz T. Aquaporin-0 membrane junctions form upon proteolytic cleavage. J Mol Biol 2004; 342:1337-45.
9. Berry V, Francis P, Kaushal S, Moore A, Bhattacharya S. Missense mutations in MIP underlie autosomal dominant 'polymorphic' and lamellar cataracts linked to 12q. Nat Genet 2000; 25:15-7.

10. Geyer DD, Spence MA, Johannes M, Flodman P, Clancy KP, Berry R, Sparkes RS, Jonsen MD, Isenberg SJ, Bateman JB. Novel single-base deletional mutation in major intrinsic protein (MIP) in autosomal dominant cataract. Am J Ophthalmol 2006; 141:761-3.
11. Jiao X, Munier FL, Iwata F, Hayakawa M, Kanai A, Lee J, Schorderet DF, Chen MS, Kaiser-Kupfer M, Hejtmancik JF. Genetic linkage of Bietti crystallin corneoretinal dystrophy to chromosome 4q35. Am J Hum Genet 2000; 67:1309-13.
12. Cottingham RW Jr, Idury RM, Schaffer AA. Faster sequential genetic linkage computations. Am J Hum Genet 1993; 53:252-63.
13. Gorin MB, Yancey SB, Cline J, Revel JP, Horwitz J. The major intrinsic protein (MIP) of the bovine lens fiber membrane: characterization and structure based on cDNA cloning. Cell 1984; 39:49-59.
14. Louis CF, Hogan P, Visco L, Strasburg G. Identity of the calmodulin-binding proteins in bovine lens plasma membranes. Exp Eye Res 1990; 50:495-503.
15. Girsch SJ, Peracchia C. Calmodulin interacts with a C-terminus peptide from the lens membrane protein MIP26. Curr Eye Res 1991; 10:839-49.
16. Nemeth-Cahalan KL, Hall JE. pH and calcium regulate the water permeability of aquaporin 0. J Biol Chem 2000; 275:6777-82.
17. Nemeth-Cahalan KL, Kalman K, Hall JE. Molecular basis of pH and Ca2+ regulation of aquaporin water permeability. J Gen Physiol 2004; 123:573-80.
18. Varadaraj K, Kumari S, Shiels A, Mathias RT. Regulation of aquaporin water permeability in the lens. Invest Ophthalmol Vis Sci 2005; 46:1393-402.
19. Yu XS, Jiang JX. Interaction of major intrinsic protein (aquaporin-0) with fiber connexins in lens development. J Cell Sci 2004; 117:871-80.
20. Yu XS, Yin X, Lafer EM, Jiang JX. Developmental regulation of the direct interaction between the intracellular loop of connexin 45.6 and the C terminus of major intrinsic protein (aquaporin-0). J Biol Chem 2005; 280:22081-90.
21. Schey KL, Fowler JG, Schwartz JC, Busman M, Dillon J, Crouch RK. Complete map and identification of the phosphorylation site of bovine lens major intrinsic protein. Invest Ophthalmol Vis Sci 1997; 38:2508-15.
22. Schey KL, Little M, Fowler JG, Crouch RK. Characterization of human lens major intrinsic protein structure. Invest Ophthalmol Vis Sci 2000; 41:175-82.
23. Lampe PD, Johnson RG. Amino acid sequence of in vivo phosphorylation sites in the main intrinsic protein (MIP) of lens membranes. Eur J Biochem 1990; 194:541-7.

The print version of this article was created on 30 Sep 2007. This reflects all typographical corrections and errata to the article through that date. Details of any changes may be found in the online version of the article.